Mechanics and Mechanical Engineering
Vol. 17, No. 1 (2013) 71–87

Post–Buckling State of Rectangular Plate Stiffened by Denselly Arranged Ribs. Numerical Analysis and Experimental Investigation

Henryk Kopecki
Łukasz Święch
Department of Aircraft and Aircraft Engines
Rzeszów University of Technology
Powstańców Warszawy 8, 35–021 Rzeszów, Poland
hkopecki@prz.edu.pl
l_swiech@prz.edu.pl

Received (10 March 2013)
Revised (17 April 2013)
Accepted (23 May 2013)

The paper presents results of comparative experimental examinations and numerical analyses of rectangular plates subjected to shear treated as a skin of half–monocoque aircraft structure. There were considered: the plate without stiffeners 2 mm thick and structure with 1 mm thickness, stiffened by 15 integral ribs. Results of nonlinear numerical FEM analyses and experimental investigations with use of 3D DIC method were compared to ones conducted for smooth plate with equivalent mass. It was documented that introduction of sub–stiffening significant influence on both the form of deformation and distribution of stress in the structure. For smooth plate low cycle fatigue test was conducted.

Keywords: Experimental investigations, FEM, post–buckling, integral structures, thin–walled structures, digital image correlation.

1. Introduction

The increasing requirements placed on the contemporary aeronautical engineering favors the intensification of the research for new structural and technological solutions aimed at minimizing the weight of aircrafts and increasing their durability and reliability at the same time.

Intensive development of mechanical processing of metals creates an opportunity for conventional materials, like aluminum alloys, to still remain one of the basic constructional materials and an increase of mentioned rate can still be seen in shaping of structure elements. The obvious sign of such tendencies is the recently intensified development of integral load-bearing aircraft structures.

The current state of knowledge in the new and intensely developing branch of engineering is best reflected in the reports compiled by order of NASA [4, 5]. The reports favors the trend in question both on account of the advantageous economic balance resulting from the possibility to eliminate the numerous labor intensive indirect assembling processes and due to the impact on the possibility to impose increasing requirements, mainly those for durability and reliability of constructions.

The development of integral structures is also favored by the intensive development of additive manufacturing technologies, popularly called 3D printing. The additive method involves the use of polymeric materials and metal powders (among other metals, titanium). These technologies allow making (printing) geometrically intricate spatial structures, while it is often unfeasible to make with use of traditional machining technologies. Application of the 3D printing method portends far–reaching optimization in terms of strength and, by extension, significant reduction in the weight of the construction.

The availability of scientific studies on issues describing the design processes and experimental study details, in particular, the prototype solutions for integral constructions, is exceptionally poor. This can be accounted for by reasons involving the confidentiality clauses widely applied by corporations that invest financial resources in long–term and expensive research processes.

Among the most recent publications, one can highlight those presenting solutions for the problem of rectangular plates with dense ribbing, subjected to compression [7, 8] and [9].

2. Research objective

The aim of the research was post–buckling behavior of integral sub–stiffened plate subjected to shear. The suggested solutions consist in using skin elements of the airframe structure in the form of integrally manufactured plates sub–stiffened with densely arranged low–profile ribs. The modification results in reduced skin thickness, equal or reduced weight of the stiffened structure compared to the unstiffened one, an increased level of buckling loads, as well as in a decrease in both the levels and gradients of effort and, consequently, in extended fatigue life of the construction.

2.1. *Plate stability*

Thin walled aircraft structures consists framework and the skin, distinguishes by it, that the skin function is limited to take over shear stress only. It is result of the trend for minimizing the mass of structure, with respect to remain required life and reliability what in fact leads to state that skin elements locally lose the stability in the range of operational loadings. This kind of deformation state isn't remaining without influence for reducing stiffness of structure, in particular torsional stiffness, what effects in nonlinear displacement and stress redistribution.

Analytical solution of such problem is quite difficult to solve. In example of plate subjected to shear with all edges fixed plate's surface is described by differential equation (1).

$$D\left(\frac{\partial^4 w}{\partial x^4} + 2\frac{\partial^4 w}{\partial x^2 \partial y^2} + \frac{\partial^4 w}{\partial y^4}\right) = 2N_{xy}\frac{\partial^2 w}{\partial x\,\partial y} \tag{1}$$

For sub–stiffened plate with variable stiffness in main directions $D = D(x, y)$ differential equation (2) is very complicated and obtaining exact analytical solution takes into account difficulty with finding appropriate function of initial deflection $w = w(x, y)$.

$$\nabla^2(\overline{D}\,\nabla^2 w) - (1-v)\left[\frac{\partial^2\overline{D}}{\partial y^2}\frac{\partial^2 w}{\partial x^2} - 2\frac{\partial^2\overline{D}}{\partial x\,\partial y}\frac{\partial^2 w}{\partial x\,\partial y}\frac{\partial^2\overline{D}}{\partial x^2}\frac{\partial^2 w}{\partial y^2}\right] = 2N_{xy}\frac{\partial^2 w}{\partial x\,\partial y} \qquad (2)$$

2.2. *Research procedure – stress field verification*

The entire research undertakings were aimed at obtaining a correct effort distribution (H–M–H stress) of the tested structures, provided that (according to the theory of elasticity) to each state of deformation correspond only one state of stress.

A hybrid numerical–experimental research methodology [2, 3] was used. The test procedure (Fig. 1) for the chosen construction began with the measurement of the geometrical deviations occurred in the manufacture stage. The use of a white light scanner in combination with a digital spatial photogrammetry system allowed creating an exact three–dimensional representation of the object, which was compared to the basic CAD geometry. Obtained deviations were introduced to the FEM model.

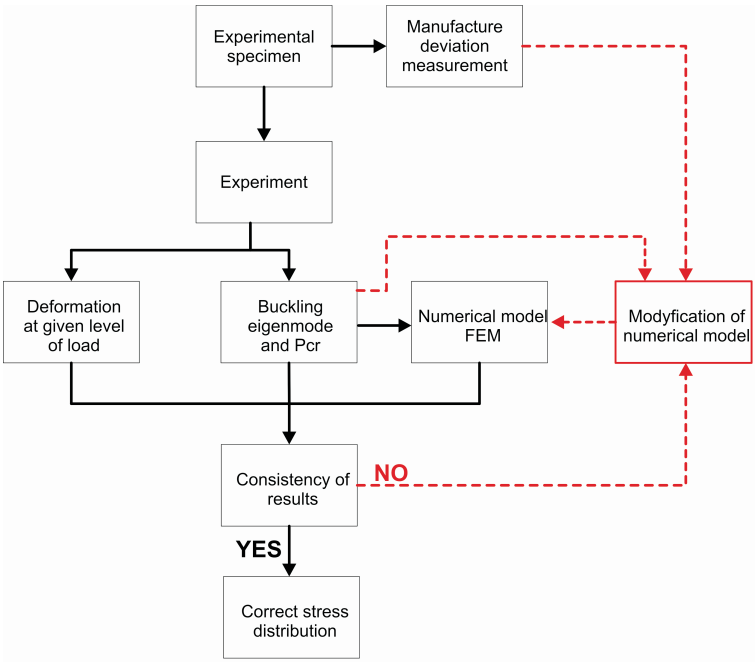

Figure 1 Validation of the obtained H–M–H stress distribution

The experimental tests were carried out on our strength testing machines that enable control of load level, and the structure deformation was kept recorded during the tests using a measuring system based on 3D digital image correlation (DIC). Buckling eigenmode and value of critical load were also recorded. Nonlinear FEM analyses were conducted at the same time.

The experiment results were compared to the results of the nonlinear numerical analyses. If there was no convergence of solutions or the convergence was inadequate, the numerical model have been modified by making alterations that result from the measured preliminary geometric imperfection recorded in the first stage of the experiment.

When numerical and experimental deformation were consisted stress distribution obtained numerically was considered as correct.

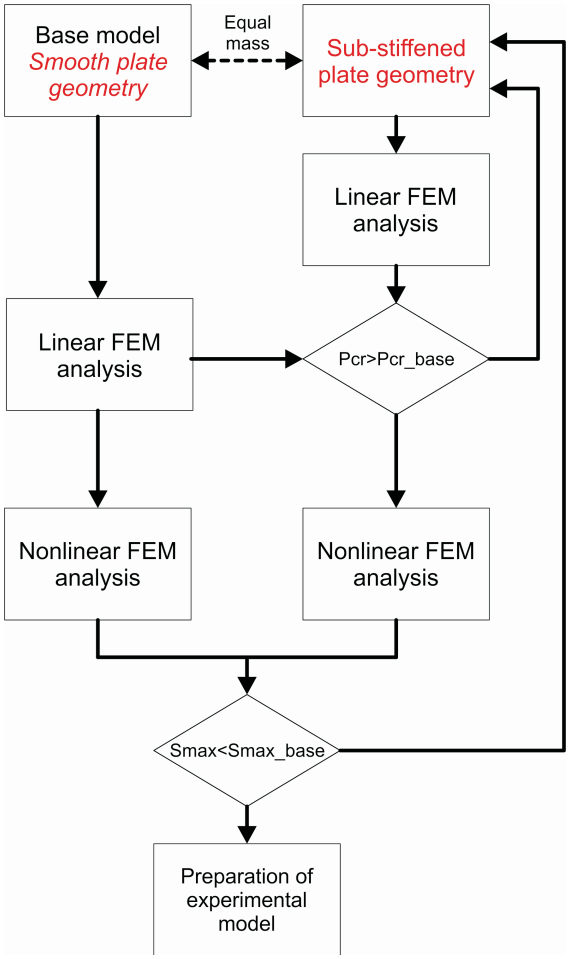

Figure 2 Sub–stiffened plate's geometry design procedure

3. Specimens

3.1. *Specimen design*

Geometry of sub–stiffened plate was designed with use of FEM solutions. As a reference geometry smooth plate was chosen. Overall dimensions for both plate were the same. Thickness of plate, geometry and number of integral ribs were designed. Goals for new structure were increasing of critical load and decreasing stress levels of the sub–stiffened plate at the same level of load, with assumption that it's mass cannot exceed mass of the reference plate. Firstly linear buckling analysis of both plates were conducted. If critical load was higher, preliminary nonlinear analyses were done, which provided stress level. Iterative process of changing geometry have been done when all assumptions have been met, then the experimental model was manufactured. Fig. 2 presents geometry design procedure.

3.2. *Chosen geometry and material of specimen*

As we mentioned above, the main subject of examination was the skin element of air bearing structure in the form of the rectangular plate, stiffened with ribs. The plate was subjected to the numerical analysis and experimental studies, for circumstance of the stability loss and post–buckling state. As a reference structure the plate without stiffeners was accepted. Both plates possessed identical measurements of 220x300 mm, at what thickness of the smooth plate was 2 mm, while alternative structure was executed as the plate about 1 mm thickness integrally stiffened by fifteen stringers about 2.5 mm width and 8 mm height (Fig. 3). Material of both plates constitutes polycarbonate about known physical characteristics. Masses of the plate without stiffeners was 208 grams, while the mass of the stiffened structure – 184 grams, i.e. it was lighter from the smooth plate about 11.5%.

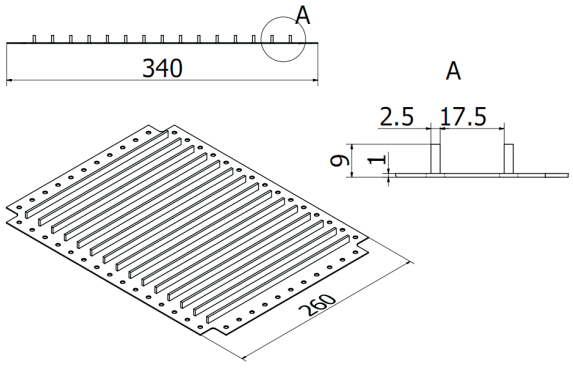

Figure 3 Geometry of sub–stiffened plate. Dimensions in mm

As a material polycarbonate polymer was chosen, for which character of stress–strain curve is very similar to aluminum alloys used in aircraft industry. Normalized series of tests were done with results of Young modulus - 2400 MPa, Poisson's ratio equal 0.36 and test yield stress was 60 MPa.

3.3. *Manufacturing process*

Experimental models were manufactured by using numerically–controlled machines: milling plotter from KIMLA (Fig. 4) and a CNC milling center from HAAS (Fig. 5).

Figure 4 Milling plotter

Figure 5 CNC milling center

Obtaining high dimension accuracy turned out to be very problematic, especially in case of sub–stiffened plate thickness.

Initially, semi–finished product in the form of polycarbonate sheet was glued and clamped to the surface of the machine working area (Fig. 6), but this way of mounting cannot provide required accuracy, probably due to strain of adhesive layer.

This problem led to construction of special vacuum table (Fig. 6) used to fix polycarbonate sheet, what ensured tight fitting of the worked detail into the table surface.

The chosen final fixing method and use of professional CNC milling center after many attempts allowed obtaining plate with dimensional tolerance reaching 0.01 mm.

Figure 6 Mounting methodes and vacum table used in manufacturing process

3.4. *Measurement of manufacture deviations*

The manufacturing accuracy of the tested sub–stiffened structure was identified with use of two different measuring methods.

Firstly measuring probe of CNC machine was used. Plate was strictly attached to vacuum table after manufacturing process. Fig. 7 presents the idea of measurement. Thickness of plate was calculated as a difference of vacuum table surface position and position of upper surface of plate. It was 48 measuring points what allows to build map of thickness distribution over plate's surface. Fig. 7 presents result of measurement for one of the first, unsuccessfully made plate.

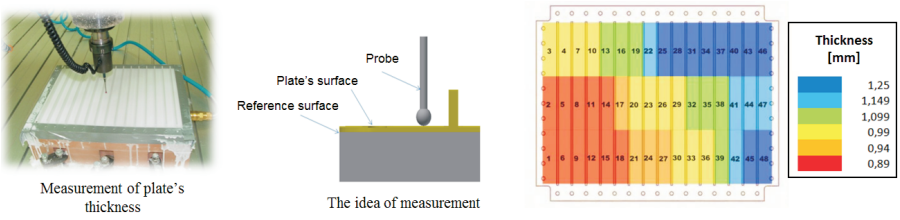

Figure 7 The idea of thickness measurement with use of CNC machine probe

The second method used was connection of the ATOS white light scanner and the TRITOP digital photogrammetry system. The set of these two latest generation gauges allows creation of digital representations of real objects. The photogrammetry system provides information on the spatial position of the so called reference

points previously placed on the object. Measuring with the use of the ATOS scanner consists in taking a series of photos of the testes object, onto which projection shadow moiré is thrown. The interference fringe pattern related to the element shape is recorded by the matrices of two stereo–metrically arranged digital cameras so that it is possible to determine the spatial position of each visible point. The resulting spatial point cloud is subjected to the so called triangulation process which results in the creation of an initial 3D digital model. The scanner software enables ordering of the set of triangles, smoothing the output surfaces and removing unnecessary elements. As a result, a model reflecting the scanned element was created (with accuracy of 0.001 mm).

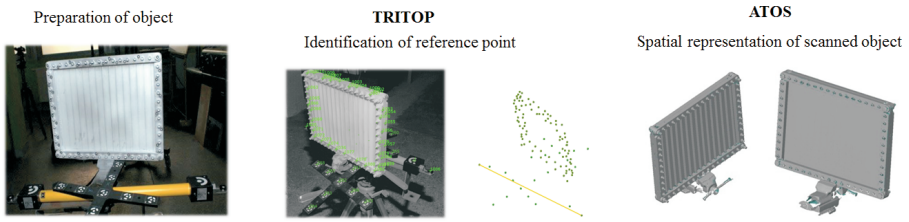

Figure 8 The idea of geometry measurment with use of spatial scanner and photogrametry system

4. Experimental procedure

Experimental tests were made with use of ZWICK Z050 strength testing machine, which ensures the possibility of control both with the force level and displacement. Testing machine was equipped with strain gauge force transducer head with 50 kN nominal size of load with the recording possibility of 0.12% of nominal force. During the experiments, it was established a steady increase in the value of force in the time of 50 N/s to the level of 6 kN what corresponds to stress level of about 60% of yield stress for smooth plate.

Plates were connected to the stiff steel frame by means of screw joints; with control of clamp force during assembly (Fig.9). Accepted method of the fastening was interpreted as a fixing. Attachment of the frame assured blocking of all degrees of freedom of lower node except from the possibility of the rotation with regard to the perpendicular axis to the surface. This node was treated as the constant support. Top node, which was place of force introduction on structure, possessed also the possibility to move upwards and down. Method of attachment and loading led to pure shear stress state on plate's edges.

4.1. *Identification of displacement fields*

Surface deformation of the tested structures was recorded with an optical scanner that applies the aforementioned three–dimensional version of the ARAMIS digital image correlation method.

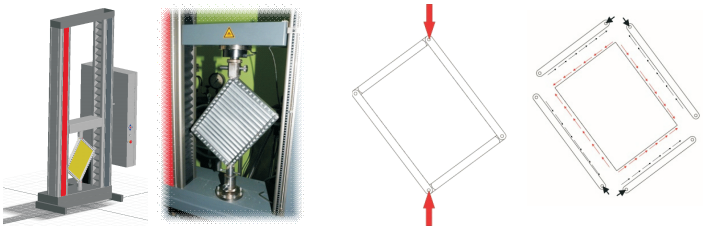

Figure 9 Attachment conditions, way of the loading and operated forces on the plate

This is an optical–numerical experimental method for spatial measurement of deformation of any shape of structure, irrespective of the object material, so that the tests can cover the real elements of the construction even while they are in use.

The measuring system consists of two high resolution digital cameras arranged to each other, so that it is possible to build a spatial image. The system can take photos at a maximum speed of 25 frames per second.

The measurement is taken on the previously prepared object. The preparatory action consists in coating the element surface with white paint followed by covering with a stochastic black dot pattern (Fig. 10).

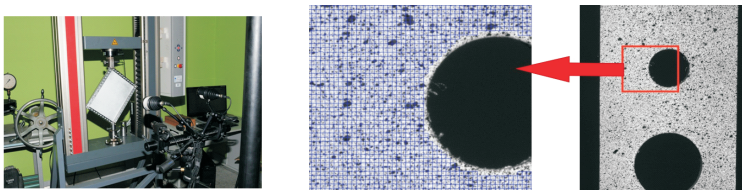

Figure 10 The plate on the research stand and surface division into strain grid

The selection of the dot size depends on the dimension of the tested object and on the optical part properties of the measuring apparatus. The surface of the tested structure is then divided into a number of elements making up a so called strain grid being a basis for further calculations. The measurement consists in taking a series of photos of the object during the consecutive phases of loading. The photos are sent to the computer software where, in the first step, the correlation of images from both the cameras enables determination of the position of every point by assigning coordinates to them in the three–dimensional reference system. The images are then divided into so called strain grids, each of which contains a unique arrangement of dots. The initial configuration becomes a reference stage. During the element loading, the dots in each element of the grid change their position relative to each other as a result of surface deformation, which is a basis for calculation of the system deformation in comparison with the reference position.

The ARAMIS device controlling the system allows reception of analogues signals in the form of voltage information (±10 V). Such a signal can be outputted from the controller of the strength testing machine so that it becomes possible to assign an adequate structure load level to each measurement phase, which allows recording of equilibrium paths during the tests by use of the force–deformation system.

5. Numerical analysis

Simultaneously with experimental examinations numerical analyses were carried out for both of considered structures. Analyses were made with use of the commercial FEM code ABAQUS, utilizing non–linear solution procedures.

5.1. *Numerical models*

Steel frame, in which plates were fixed was modeled by means of three–dimensional, two node beam elements B31, with six degree of freedom in each node. Articulated connection of the frame elements were modeled using three–dimensional link elements CONN3D2 of the HINGE type. In order to represent the montage in handles of the strength test machine lower node of the frame was fixed, however to the top node concentrated force was applied, leaving the possibility of movement in direction of force working.

Plates and ribs were modeled using three–dimensional, four nodes shell elements S4R with six degree of freedom in each node and reduced number of integration points on the surface of the element. This type of element is recommended in cases of big deformation analyses and ensures the possibility of thickness change during increase of deformation. In considered problem, five integration points were applied through the thickness of the element. In the purpose of compensation influence of reduced integration point's number Hourglass control was also applied.

Connection of the frame to plate was being realized through the fixed combination of the TIE constraint of the ABAQUS program library, making the assumption that any slip between these elements does not occur. In the identical way ribs were being linked to the surface of the plate. Geometry of models together with the division into finite elements mesh is presented on the Fig. 11.

In the first order the linear analysis of the plate stability were made. Results of this kind of analysis were eigenmode deformations and values of critical load.

5.2. *Nonlinear analyses*

Desired stress levels of researched structures are possible to obtain only by means of nonlinear algorithms of FEM [1]. Nonlinear stability analyses of the plate without stiffeners are possible exclusively after introducing initial geometric imperfection, assumed in the form of the plate preliminary deflection in neutral state. So state were obtained through applying the IMPERFECTION command added to the ABAQUS input file, adjusting initial geometry to suitably rescaled forms of buckling obtained on the way of the linear analyses of stability.

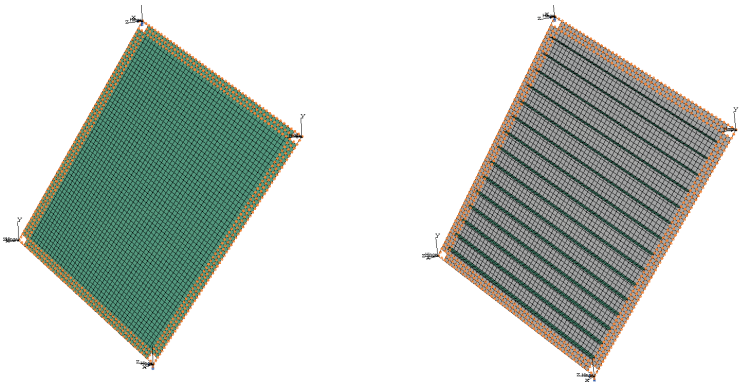

Figure 11 Numerical models of plates with FEM mesh

Nonlinear analyses were carried out applying the modified Riks method taking advantage Newton's – Raphson procedure, belonging to family of arc–length method. In this procedure the value of the loading, represents the extra variable, and so it is necessary to accept another parameter to control of the solution. In the ABAQUS environment it is a length of the arch along static equilibrium path.

6. Results

This section presents results of researches divided into two subsections. First one contains comparisons of experimental and numerical results, second leads to conclusions made by analysis of sub–stiffened plate behavior in range of post critical loading.

6.1. *DIC vs. FEM*

6.1.1. *Smooth plate*

As the referential solution, results of experimental studies were accepted executed by means of the scanner ARAMIS. Fig. 12 documents equilibrium path for smooth plate, made for point of maximal value of deflection, in the geometrical center of plate's surface. It was observed good agreement in full range of loading applied during experimental investigations.

Fig. 13 presents deflection field's comparison of FEM and DIC results. Maximal deviation was at level of 0.16 mm (about 5.4%). It is worth noting that form of deformation was almost perfectly agreed for every point of plate's surface.

In case of smooth plate it was possible to obtain stress distribution by adding material properties to the ARAMIS software. Fig. 14 presents stress fields for both FEM and DIC results.

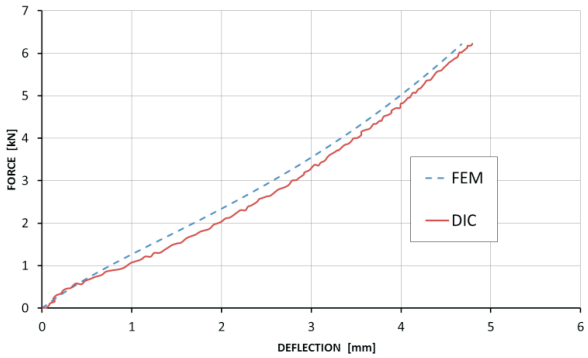

Figure 12 Representative equilibrium path for smooth plate, for point of maximal value of deflection

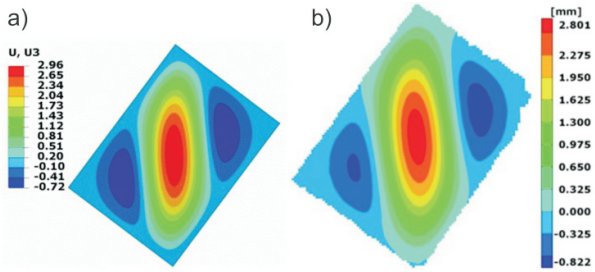

Figure 13 Deflection field of smooth plate. Load 3 kN. (a) FEM result; (b) DIC one

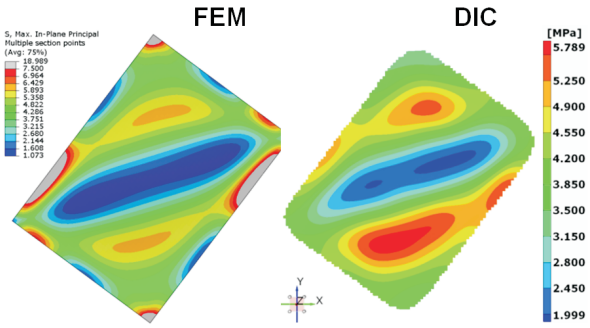

Figure 14 Major stress field for smooth plate

6.1.2. *Stiffened plate*

Comparison of deflection's patterns obtained by numerical and experimental analyses of stiffened plate presents Fig. 15. Small differences in shape of deformation between results are consequences of manufacturing errors and initial geometrical imperfection of plate surface from mounting into the frame, which were not exactly included into numerical model. However, for higher levels of load paths were convergent.

Fig. 16 shows deflection fields in the state of post–critical deformation in final stage of loading at level of 6 kN. Presented distributions point on the almost perfect agreement in both the shape and values of deflections.

Introduction of ribs on the surface of sub–stiffened plate made it impossible to acquire stress field for DIC results. Fig. 17 presents comparison of major strain field. Both results were on equal levels.

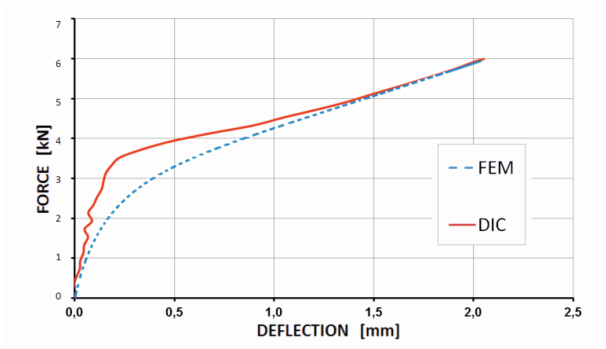

Figure 15 Representative equilibrium path for sub–stiffened plate, for point of maximal absolute value of deflection

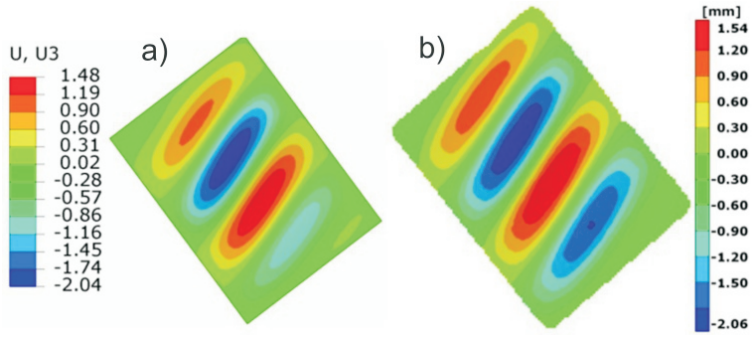

Figure 16 Deflection field of sub–stiffened plate. View from unstiffened side. (a) FEM result; (b) DIC one

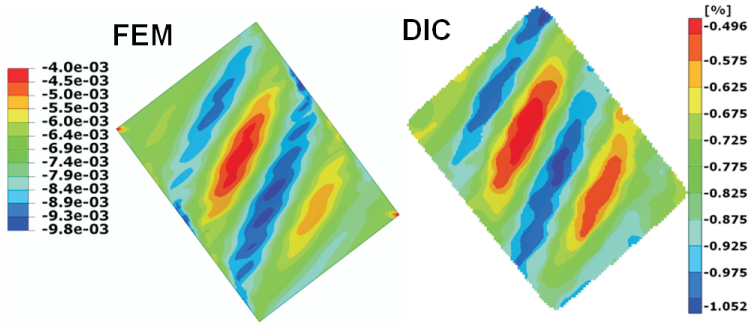

Figure 17 Major strain fields

6.2. *Comparison of results for plate*

Good agreement in deformation of examined plates compared to experimental results gives the possibility to assume that stress fields obtained by FEM analyses are correct. Fig. 18 shows comparison of H–M–H stress distribution over the surface of tested structures. Obtained results points on substantial decrease in gradient of effort with no increasing its level (Fig. 18), what could have significant meaning for fatigue life of structure.

Obtained results indicate the significant change in the form of buckling (Fig. 13 and Fig. 16); from one to four half waves, with maximal magnitude decreased about 50 % compared to smooth plate.

Sub–stiffened plate's buckling load was 50 % higher than result for smooth one.

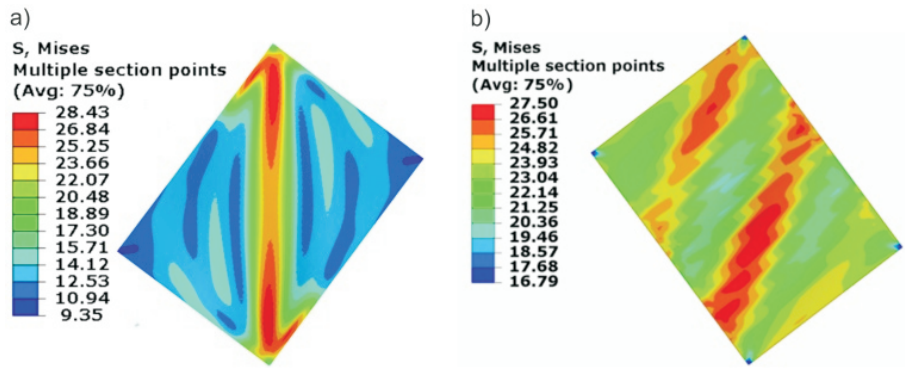

Figure 18 H–M–H stress (a) smooth plate; (b) sub-stiffened plate

7. Low cycle fatigue experimental analysis

For smooth plate experimental low cycle fatigue test was carried out. ZWICK Z050 was used with controlling of load level. Adopted load spectrum on set of monocycles from 10 N to 6000 N was based.

Fig. 19 presents location first fatigue cracks observed after about 45 000 cycles of loading. These locations covers with places of maximal effort pointed out in the result of FEM analysis, what leads to conclusion that numerical model and its boundary conditions were correct.

Four cracks on diagonal of plate appeared after 60 000 cycles and propagate to the fracture of specimen at number of 84 658 cycles (Fig. 20). After about 83 000 cycles some of cracks had length of 50 mm and did not influence on overall stiffness of the plate.

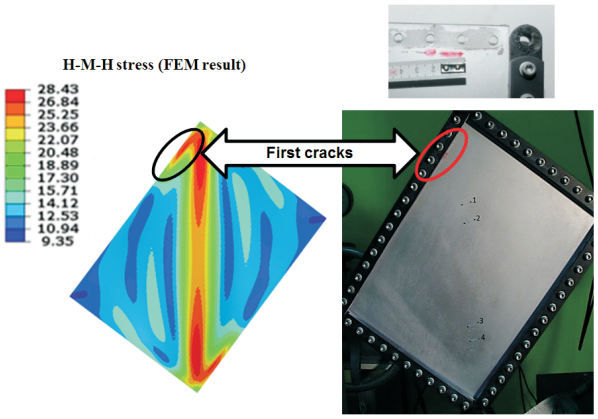

Figure 19 First fatigue cracks – 45 000 cycles of loading

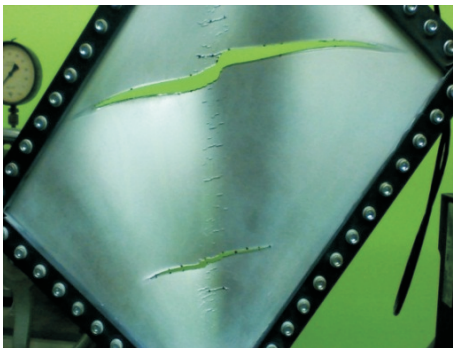

Figure 20 Fracture of plate – 84 658 cycles of loading

8. Conclusions

Result of researches shows significant impact of sub–stiffening's introduction on operational properties of thin–walled structures in post–buckling states of deformations. Presented configuration of ribs and skin thickness allows increasing buckling load for 50% and decreasing effort gradient by 40% without increasing the weight of structure.

Obtained results suggest for further investigations with other configurations and geometry of stiffeners.

Moreover adopted research methodology allows to obtain high convergence of numerical solutions for the whole range of loads, to which the construction is subjected during the experiment, and to assess the solution obtained for the initial (ideal–CAD) geometry so that it is possible to determine the confidence interval for the preliminary numerical analyses of constructions with similar geometries, which materially translates into the long–term nature and expensiveness of research on other structural solutions.

As mentioned in section 3.3 initial mounting conditions during manufacturing processes led to inaccurate fabrication. Fig. 21 presents deformation of sub-stiffened plate with thickness of 0.6 mm. Obtained results indicated that very small thickness in relation to the stiffness of the ribs causes local skin buckling between stiffeners what runs to plastic strains and collapse of the structures for relatively low levels of load.

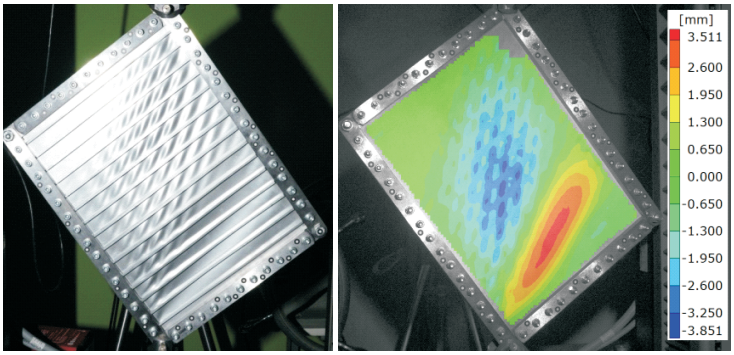

Figure 21 Post critical feformation of sub–stiffened plate with thickness of 0.6 mm

References

[1] **ABAQUS/CAE User's Manual**, Dassault Systems, **2010**.

[2] **Kopecki, H., Święch, Ł. and Zacharzewski, J.**:Analiza porównawcza wyników obliczeń numerycznych oraz badań doświadczalnych metodą cyfrowej korelacji obrazu pasma płytowego z wykrojami, *Journal of Aeronautica Integra*, 10, 35–38, **2011**.

[3] **Kopecki, H., Święch, Ł. and Zacharzewski J.**: Comparative analysis of the stress states obtained as results of numerical calculations and experimental investigations

with 3D digital image correlation method, Static, *Dynamics and Stability of Structural Elements and Systems*, A series of monographs, Łódź, 427–446, **2012**.

[4] **Munroe, J., Wilkins, K. and Gruber, M.**: Integral airframe structures (IAS)–validated feasibility study of integrally stiffened metallic fuselage panels for reducing manufacturing costs, *NASA/CR–2000–209337*, **2000**.

[5] **Metschan, S.**: Validated feasibility study of integrally stiffened metallic fuselage panels for reducing manufacturing costs, cost assessment of manufacturing/design concept, *NASA/CR–2000–209343*, **2000**.

[6] **Paulo, R., Teixeira–Dias, F. and Valente, R.**: Numerical simulation of aluminium stiffened panels subjected to axial compression: Sensitivity analyses to initial geometrical imperfections and material properties, *Thin–Walled Structures,* 62, 65–74, **2013**.

[7] **Quinn, D., Murphy, A., McEwan, W., Lemaitre, F.**: Stiffened panel stability behavior and performance gains with plate prismatic sub–stiffening, *Thin–Walled Structures*, 47, 1457–1468, **2009**.

[8] **Quinn, D., Murphy, A., McEwan, W. and Lemaitre, F.**: Non–prismatic sub–stiffening for stiffened panel plates – Stability behavior and performance gains, *Thin–Walled Structures*, 48, 401–413, **2010**.